

Nonlinear viscoelastic dynamics of nano-confined water

Tai-De Li and Elisa Riedo

School of Physics, Georgia Institute of Technology, Atlanta, GA 30332, USA

(Dated: February 1, 2008)

The viscoelastic dynamics of nano-confined water is studied by means of atomic force microscopy (AFM). We observe a nonlinear viscoelastic behavior remarkably similar to that widely observed in metastable complex fluids. We show that the origin of the measured nonlinear viscoelasticity in nano-confined water is a strain rate dependent relaxation time and slow dynamics. By measuring the viscoelastic modulus at different frequencies and strains, we find that the intrinsic relaxation time of nano-confined water is in the range $0.1 - 0.0001$ s, orders of magnitude longer than that of bulk water, and comparable to the dielectric relaxation time measured in supercooled water at $170 - 210$ K.

PACS numbers:

Confined fluids exhibit unique structural, dynamical, electrokinetic, and mechanical properties that are different from those of the bulk [1, 2, 3, 4, 5, 6, 7]. Their behavior depends on the degree of confinement, strain rate, temperature, fluid molecular structure, and interactions with boundaries. Surprising effects have been found when water is confined in nanogaps. For example, the electric field induced freezing of water at room temperature [8] and the extremely high viscosity of water close to a mica surface [1, 2, 9]. Previous experiments and calculations have pointed out the key role of the confining surfaces [1, 4]. A notable increase in viscosity and decrease in the diffusion constant was measured only when water was confined between hydrophilic surfaces. For hydrophobic confinement, the observed increase of viscosity was not very pronounced. Intriguingly, a similar behavior has been observed in confined glassy materials. When a glass-forming fluid is cooled down to the glass transition temperature, T_g , its viscosity grows by many orders of magnitude, and the confinement can increase or decrease T_g for strong or weak interactions with the walls, respectively [7].

So far, the viscosity measurements for nano-confined water have been performed in the linear viscoelastic regime. However, as observed in *macroscopic* rheological measurements, the study of the viscoelastic properties as a function of shear amplitude and rate is important for a better understanding of the dynamical and structural properties of fluids [10].

In this letter, we investigate the viscoelastic response of nano-confined water, as a function of shear amplitude and rate, by means of direct high-resolution AFM measurements. We observe a nonlinear viscoelastic behavior remarkably similar to that widely observed in metastable complex fluids, such as gels and supercooled liquids [10, 11]. We show that the origin of this nonlinear viscoelasticity in nano-confined water is a strain rate dependent relaxation time and slow dynamics. By measuring the viscoelastic modulus at different frequencies and strains, we find that the intrinsic relaxation time,

τ_0 , of nano-confined water is in the range $0.1 - 0.0001$ s, orders of magnitude longer than that of bulk water, and comparable to the dielectric relaxation time measured in supercooled water at $170 - 210$ K. [12].

In our AFM experiments [1, 13], a nano-size spherical silicon tip is brought quasi-statically to the vicinity of a flat freshly tape-cleaved hydrophilic mica surface, all immersed in purified water, while small lateral oscillations are applied to the cantilever support [1]. The normal and lateral forces acting on the tip are measured directly and simultaneously as a function of the water film thickness, i.e., tip-sample distance, d . The zero distance, $d = 0$, is where the normal force diverges.

The experiments were performed with a Molecular Imaging PicoPlus AFM. An instrumental problem in quasi-static force measurements is that, during the tip-sample approach, the tip snaps into contact with the surface at a distance where the gradient of the tip-sample forces exceeds the cantilever normal spring constant, k_N [14, 15]. To overcome this problem, we employed relatively stiff cantilevers. We used silicon tips with radii $R = 40 \pm 10$ nm and Ultrasharp NSC12/50 cantilevers with normal and lateral spring constant in the range $k_N = 3 - 4.5$ N/m and $k_L = 50 - 120$ N/m, respectively. Due to the mechanical stability of our apparatus, and a judicious choice of the cantilever stiffness [1], we are able to measure the tip-surface distance with sub-Angstrom resolution all the way down to the last adsorbed water layer. The calibration and force detection was performed as described in [13, 16]. The approach velocity was 0.2 nm/s. During the approach, lateral oscillations parallel to the mica surface were applied to the cantilever holder by means of a lock-in amplifier. The same lock-in amplifier was then used to measure the amplitude of the lateral force, F_L , and the phase difference, θ , between the applied lateral displacement and the detected lateral force. The zero of phase was chosen when the tip was in hard contact with the mica surface, for lateral oscillation amplitudes, X_0 , small enough to guarantee an elastic contact without slippage [17]. In order

to shear parallel to the mica surface, before each measurement we tilted the stage that holds the sample until the differences in height of the mica surface topography across an area of $1 \times 1 \mu\text{m}^2$ (as obtained from AFM sample topography imaging) were smaller than 1 nm. This corresponds to an angle $< 0.06^\circ$ between the mica surface and the tip shearing.

All the experiments were performed at 300 K in high purity DIUF water from Fisher Chemicals (pH = 6.1). The purity of water used in our AFM liquid cell was tested after the experiment by gas chromatography - mass spectrometry (GC-MS). GC-MS spectra of used, and not previously used, water samples were taken by 70SE spectrometer (VG Instruments). In both cases the results showed that any small molecular weight (less than 700 Da) organic contaminants were present at amounts below the instrumental threshold (5 ppm).

When a viscoelastic material is confined between two parallel plates separated by d , with area A , and a sinusoidal strain is applied to one of the plates at the frequency ω , $\gamma = \gamma_0 \sin(\omega t)$, the resulting stress between the plates can be written as $\sigma = \sigma_0 \sin(\omega t + \theta)$. The relationship between the strain amplitude, $\gamma_0 = \frac{X_0}{d}$, and the stress amplitude, $\sigma_0 = \frac{F_L}{A}$, is given by the following equation:

$$\frac{F_L}{A} = |G^*| \frac{X_0}{d} \quad (1)$$

where G^* is the viscoelastic modulus. The viscoelastic modulus contains information about the dissipative and elastic response of the confined material. In particular, G^* can be written as a complex sum of the storage modulus, G' , and the loss modulus, G'' , i.e., $G^* = G' + iG''$, as [18]:

$$G' = \frac{F_L d}{A X_0} \cos \theta, \quad G'' = \frac{F_L d}{A X_0} \sin \theta \quad (2)$$

For a purely elastic solid, σ and γ remain in phase, $\theta = 0$, and so $G'' = 0$ and $G' = G^*$.

In order to study the viscoelastic behavior of nano-confined water we have measured the lateral force and the phase when we oscillate laterally the AFM cantilever holder. As a first approximation we have assumed that the lateral spring constant of our silicon cantilever is much larger than the lateral tip-water contact stiffness for $d < 1$ nm [19]. As a consequence, we can consider that the applied oscillation amplitude to the cantilever holder is equal to the shear amplitude of the tip apex. Figure 1 shows F_L and θ as a function of d for three different shear amplitudes at a fixed shear frequency, $\omega = 955.3$ Hz. For tip-sample distances larger than 1 nm we observe that the lateral force is equal to zero within the instrumental error for any shear amplitude. As soon as $d < 1$ nm we observe that F_L increases with decreasing d , and diverges at $d = 0$ nm when the tip is in hard contact with

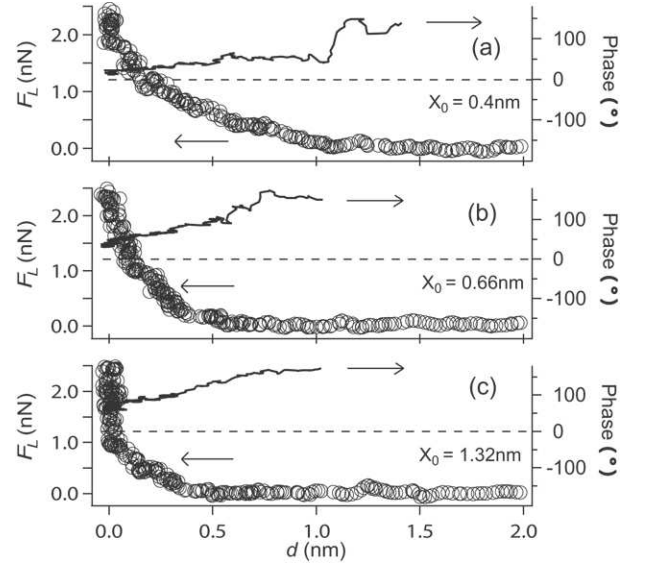


FIG. 1: The lateral force and phase as a function of tip-sample distance at constant shear frequency, 955.3 Hz, and for three different shear amplitudes, (a) $X_0 = 0.4$ nm. (b) $X_0 = 0.66$ nm. (c) $X_0 = 1.32$ nm. The phase for $d > 1$ nm is not shown because it largely fluctuates in a random way.

the mica surface. In a previous study [1], F_L has been used to calculate the viscosity of water (η) by using Eq. 1, and by considering water as purely viscous, that is, by making the approximation $|G^*| \approx G'' \approx \eta \cdot \omega$. This approximation is true when $\theta \cong 90^\circ$, which, as we show later, is the case for large strain rate amplitudes defined as $\dot{\gamma}_0 \equiv \gamma_0 \cdot \omega$. However, the phase measurements presented in Fig. 1 show that in general the behavior of nano-confined water is viscoelastic, and furthermore, we observe that the lateral force does not grow proportionally with the shear amplitude, nor with the shear frequency (not shown here). This is an indication that the viscoelastic response is not linear, and the viscoelastic modulus is shear amplitude dependent, $G^* = G^*(\gamma_0)$. Therefore, a detailed study of G^* as a function of γ_0 is needed to shed light into this nonlinear behavior.

By applying Eq. 2 to the data in Fig. 1, we have extracted G' and G'' as a function of d for different X_0 at a fixed ω . (The A used for Eq. 2 is the contact area corresponding to the spherical segment defined by the intersection between the spherical tip and a plane at $z = d + \Delta h$, $\Delta h = 0.25$ nm, i.e., a water molecule diameter [1].) Figure 2 shows very clearly that G' and G'' strongly depend on the shear amplitude. G'' dominates over G' for large shear amplitudes, where the response of nano-confined water becomes purely viscous. Also, by decreasing the gap size, we observe that the rise of G' and G'' takes place *later* (smaller d) for larger shear amplitudes. Furthermore, for all the investigated shear amplitudes, the rise of G'' occurs *earlier* (larger d) than the onset of G' . The dramatic drop of both G' and G'' for $d < 0.2$ nm

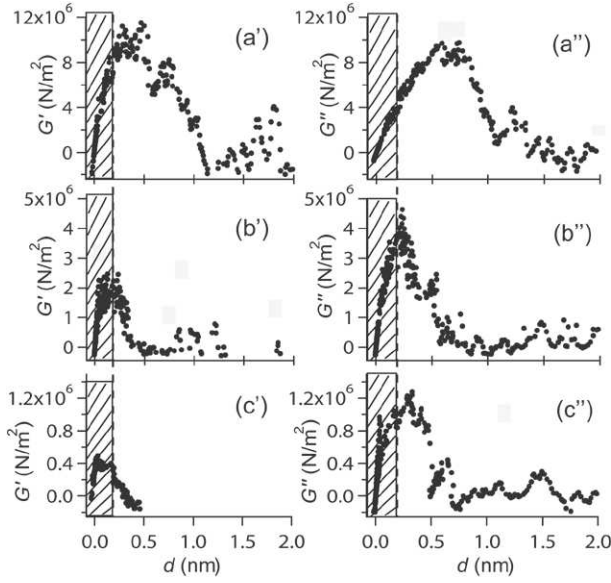


FIG. 2: G' and G'' as a function of tip-sample distance. The shadowed area, $d < 0.2$ nm, is not discussed in this letter because the gap size is smaller than a water molecular dimension. The frequency is 955.3 Hz, and the shear amplitude is 0.4 nm for (a') and (a''), 0.66 nm for (b') and (b''), and 1.32 nm for (c') and (c'').

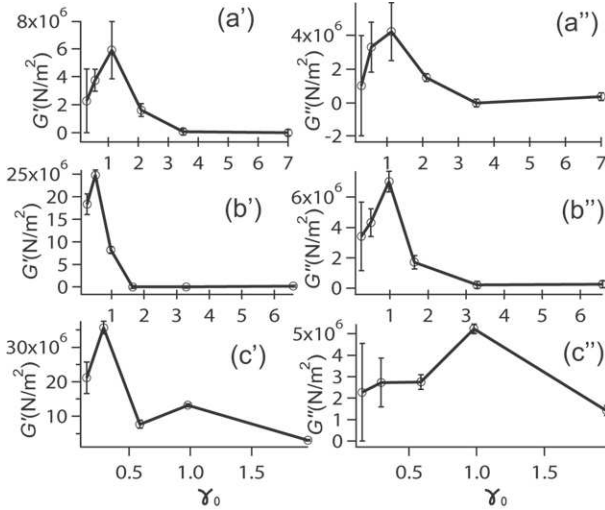


FIG. 3: At a constant distance, $d = 0.4$ nm, G' and G'' as a function of $\gamma_0 = \frac{X_0}{d}$. The shear frequency is 52.02 Hz for (a') and (a''), 955.3 Hz for (b') and (b''), and 1.9689 kHz for (c') and (c'').

(shadowed area in Fig. 2) is due to the invalidity of Eq. 2 for distances smaller than the dimension of one water molecule. Figure 2 indicates that the shear amplitude dependence of the viscoelastic modulus is very complex and nonlinear. For this reason we have performed measurements over a large range of shear amplitudes and frequencies ($0.06 \text{ nm} < X_0 < 2.8 \text{ nm}$, $50 \text{ Hz} < \omega < 2 \text{ kHz}$).

Following the Maxwell model for a linear viscoelastic

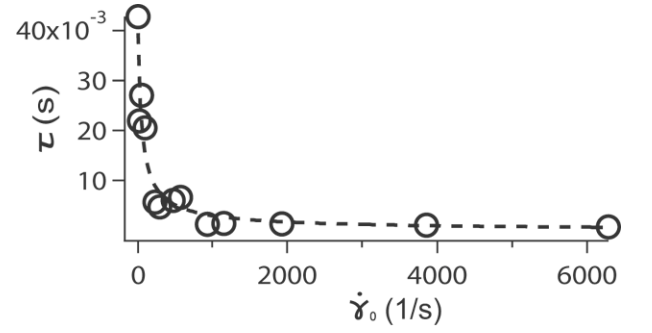


FIG. 4: The effective relaxation time as a function of $\dot{\gamma}_0 = \gamma_0 \cdot \omega$ at $d = 0.4$ nm. The dash line is the fitting with Eq. 4.

system, the relationship between the intrinsic relaxation time, τ_0 , and the moduli, G' and G'' , is given by [18]

$$G' = \frac{G_0(\omega\tau_0)^2}{1 + (\omega\tau_0)^2}, \quad G'' = \frac{G_0(\omega\tau_0)}{1 + (\omega\tau_0)^2} \quad (3)$$

where G_0 is a constant. According to Eq. 3, G' and G'' do not depend explicitly on γ_0 . However, many complex fluids experience a drastic decrease of their structural relaxation time when they are subjected to large strains. This phenomenon gives rise to a strong strain dependence of G' and G'' , which can be described by the introduction of an *effective* relaxation time τ that depends on the *intrinsic* relaxation time and the strain rate [10]. Once defined τ , it is used to replace τ_0 in Eq. 3, and thus to predict G' and G'' as a function of the strain. Recently, a phenomenological expression has been found to characterize a strain dependent effective relaxation time [10]

$$\frac{1}{\tau} \simeq \frac{1}{\tau_0} + K \cdot \dot{\gamma}_0^\nu \quad (4)$$

where ν is a positive exponent, and K is a constant. In a glassy system which shows slow dynamics ($\omega \gg \frac{1}{\tau_0}$), $\nu \sim 1$ and $K \sim 1$ [20, 21]. By replacing τ_0 in Eq. 3 with τ in Eq. 4 when $\omega \gg \frac{1}{\tau_0}$, the maximum of G'' is near $\gamma_0 \simeq 1$, independently of the frequency. Figure 3 presents G' and G'' vs. γ_0 for nano-confined water, obtained by applying Eq. 2 to the measured F_L and θ at three different frequencies for $d = 0.4$ nm. G' and G'' in Fig. 3 show remarkable behavior: (i) the peak position of G'' is around $\gamma_0 \simeq 1$ over a wide range of frequencies; (ii) for $\gamma_0 < 1$, the viscoelasticity is dominantly elastic, i.e., $G' > G''$; and (iii) G' and G'' decay to zero for large values of γ_0 . These features of our nano-confined water system are ubiquitous in metastable complex fluids [10] and they are captured by the argument of the strain rate dependent effective relaxation time. Indeed, by using Eq. 3 and 4 the shape of the curves presented in Fig. 3 can be fully described.

From Eq. 3, the effective relaxation time can be pre-

dicted by:

$$\tau = \frac{G'}{G''} \cdot \frac{1}{\omega} \quad (5)$$

By using Eq. 5 and the experimental values of G' and G'' , τ as a function of $\dot{\gamma}_0$ for $d = 0.4$ nm is determined and shown in Fig. 4. The effective relaxation time of nano-confined water decreases from 40 ms to 0.7 ms when the strain rate increases from 14 s^{-1} to 6000 s^{-1} . The nonlinearity of the relaxation time sets in when the experimental time scale ($\dot{\gamma}_0$) is faster than the intrinsic relaxation time (τ_0). In this case, the time response can only be measured effectively as a function of the experimental time scale.

By fitting the data in Fig. 4 with Eq. 4 we found that the intrinsic relaxation time was $\tau_0 = 0.06 \pm 0.03$ s for $K = 0.95 \pm 1.49$ and $\nu = 0.84 \pm 0.29$. These values of ν and K are similar to those found in complex metastable fluids with slow dynamics [20, 21]. The striking result is that the observed τ and τ_0 are orders of magnitude slower than the relaxation time of bulk water at room temperature, which is of the order of 10^{-12} s. The fact that confinement can drastically slow down the dynamics of a fluid has been previously observed in diverse systems, such as colloidal suspensions [22] and polymers [5], where for strong fluid-wall interactions, the glass transition temperature is shifted towards high temperatures upon confinement [7]. An alternative way to view this behavior is to consider that the confinement defines an effective temperature of the system which is lower than the canonical temperature. According to a previous study [12], the dielectric relaxation time of supercooled water confined in clays at 175 K is about 0.06 s similar to the relaxation time found in our experiments on nano-confined water at room temperature. Moreover, the value of the viscosity measured in our investigations is comparable with that of supercooled water at 140 K in a $100 \mu\text{m}$ radius tube [23]. A recent study has shown that the dielectric relaxation time of supercooled water is very sensitive to the confinement [24]. For confinement lengths of the order of 1 nm, it was found that, over a wide range of temperatures, the dielectric relaxation times are always longer than in bulk water. In our experiments, we also observe that τ decreases with reduced confinement, i.e., with increasing d . Unfortunately, for $d \geq 1$ nm the lateral force becomes so small that we cannot measure its value precisely due to low signal-to-noise ratio. The only information that we can extract is that the intrinsic relaxation time for $d \geq 1$ nm is shorter than 10^{-4} s.

In conclusion, we have studied the room temperature viscoelastic properties of nano-confined water, finding a slow dynamical behavior similar to that observed in metastable complex fluids. By measuring the viscoelastic modulus at different frequencies and strains, we have found that the intrinsic relaxation time of nano-confined water is about 0.06 s. This value is comparable with the

dielectric relaxation time measured in supercooled water at 175 K.

We thank H. M. Wyss and L. Bocquet for helpful discussions. We gratefully acknowledge the financial support of the NSF DMR-0405319, DOE DE-FG02-06ER46293 and NSF STC grants.

-
- [1] T.-D. Li, J. Gao, R. Szożkiewicz, U. Landman, and E. Riedo, *Phys. Rev. B* **75** (2007).
 - [2] M. Antognozzi, A. Humphris, and M. Miles, *Appl. Phys. Lett.* **78**, 300 (2001).
 - [3] S. Jeffery, P. M. Hoffmann, J. B. Pethica, C. Ramanujan, H. O. Ozer, and A. Oral, *Phys. Rev. B* **70** (2004).
 - [4] T. Uchihashi, M. Higgins, Y. Nakayama, J. Sader, and S. Jarvis, *Nanotechnology* **16**, S49 (2005).
 - [5] M. Alcoutlabi and G. B. McKenna, *J. of Phys.: Cond. Matt.* **17** (2005).
 - [6] R. C. Major, J. E. Houston, M. J. McGrath, J. I. Siepmann, and X.-Y. Zhu, *Phys. Rev. Lett.* **96** (2006).
 - [7] P. Scheidler, W. Kob, and K. Binder, *Europhys. Lett.* **59**, 701 (2002).
 - [8] E.-M. Choi, Y.-H. Yoon, S. Lee, and H. Kang, *Phys. Rev. Lett.* **95** (2006).
 - [9] Y. Zhu and S. Granick, *Phys. Rev. Lett.* **87**, 096104 (2001).
 - [10] K. Miyazaki, H. M. Wyss, D. A. Weitz, and D. R. Reichman, *Europhys. Lett.* **3** (2006).
 - [11] M. D. Ediger, C. A. Angell, and S. R. Nagel, *J. Phys. Chem.* **100** (1996).
 - [12] S. Cervený, G. A. Schwartz, R. Bergman, and J. Swenson, *Phys. Rev. Lett.* **93**, 245702 (2004).
 - [13] R. Szożkiewicz and E. Riedo, *Phys. Rev. Lett.* **95**, 135502 (2005).
 - [14] U. Raviv, P. Laurat, and J. Klein, *Nature* **413**, 51 (2001).
 - [15] S. O'Shea and M. Welland, *Appl. Phys. Lett.* **60**, 2356 (1992).
 - [16] R. Lüthi, E. Meyer, H. Haefke, L. Howald, W. Gutmansbauer, M. Guggisberg, M. Bammerlin, and H.-J. Güntherodt, *Surf. Sci.* **338**, 247 (1995).
 - [17] R. W. Carpick, D. F. Ogletree, and M. Salmeron, *Appl. Phys. Lett.* **70**, 24 (1997).
 - [18] J. D. Ferry, *Viscoelastic Properties of Polymers* (Wiley, 1980), 3rd ed., ISBN 0-471-04894-1.
 - [19] From the results in Fig. 2, the shear elastic modulus of nanoconfined water, G' , is three orders of magnitude smaller than the shear modulus of silicon, $G^s \simeq 50$ GPa. The tip-water contact lateral stiffness is approximately equal to $K_L^c \sim 8a(\frac{1}{G'} + \frac{1}{G^s})^{-1} \sim 0.4$ N/m, (a is the contact radius, $a \simeq 4.5$ nm in these experiments), which is two orders of magnitude smaller than the torsion and lateral force constant.
 - [20] K. Miyazaki and D. R. Reichman, *Phys. Rev. E* **66** (2002).
 - [21] K. Miyazaki, D. R. Reichman, and R. Yamamoto, *Phys. Rev. E* **70** (2004).
 - [22] C. R. Nugent, H. N. Patel, and E. R. Weeks, *arXiv:cond-mat/0601648v1* (2007).
 - [23] J. Hallett, *Proc. Phys. Soc. of London* **82** (1963).
 - [24] J. Swenson, H. Jansson, and R. Bergman, *Phys. Rev. Lett.* **96**, 247802 (2006).